The connection between the star formation and the supernova remnants

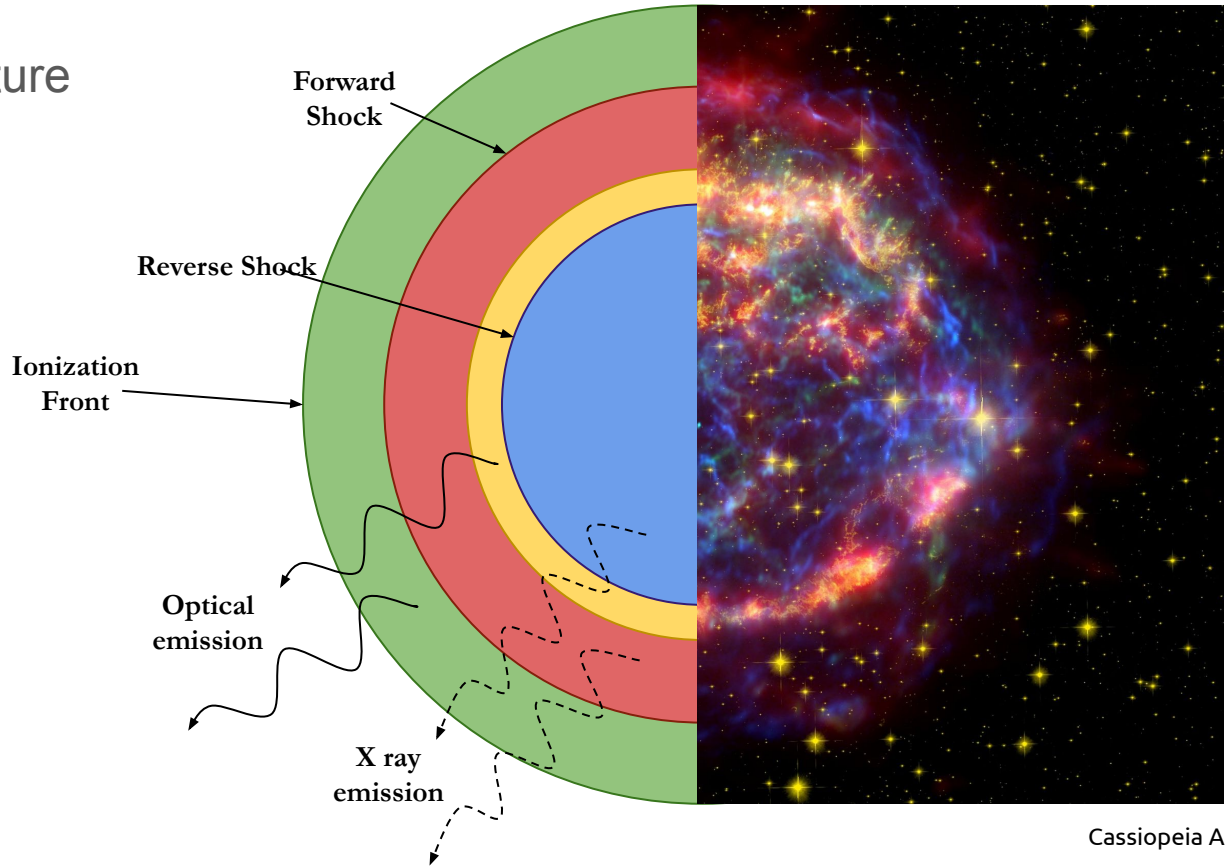
A path from the supernovae rate in the nearby universe to the shocked and enriched interstellar medium and back

Asier Castrillo

Structure

Supernova Remnants

Structure



Cassiopeia A

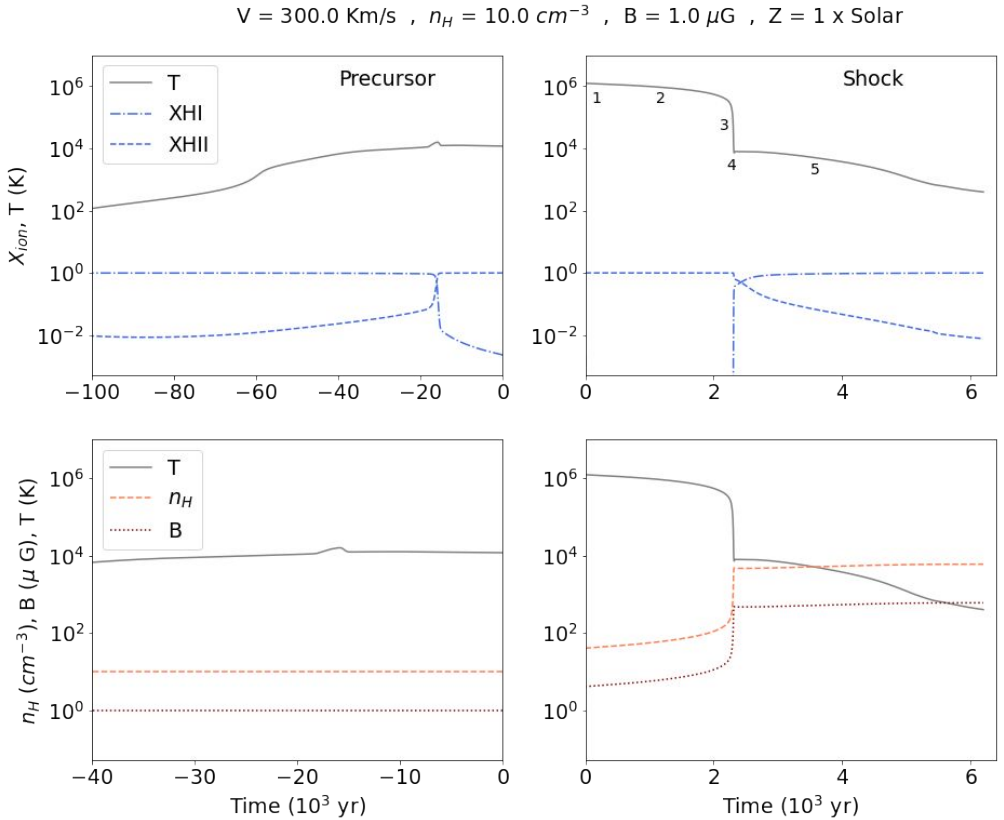
MAPPINGS models

R-type Shocks

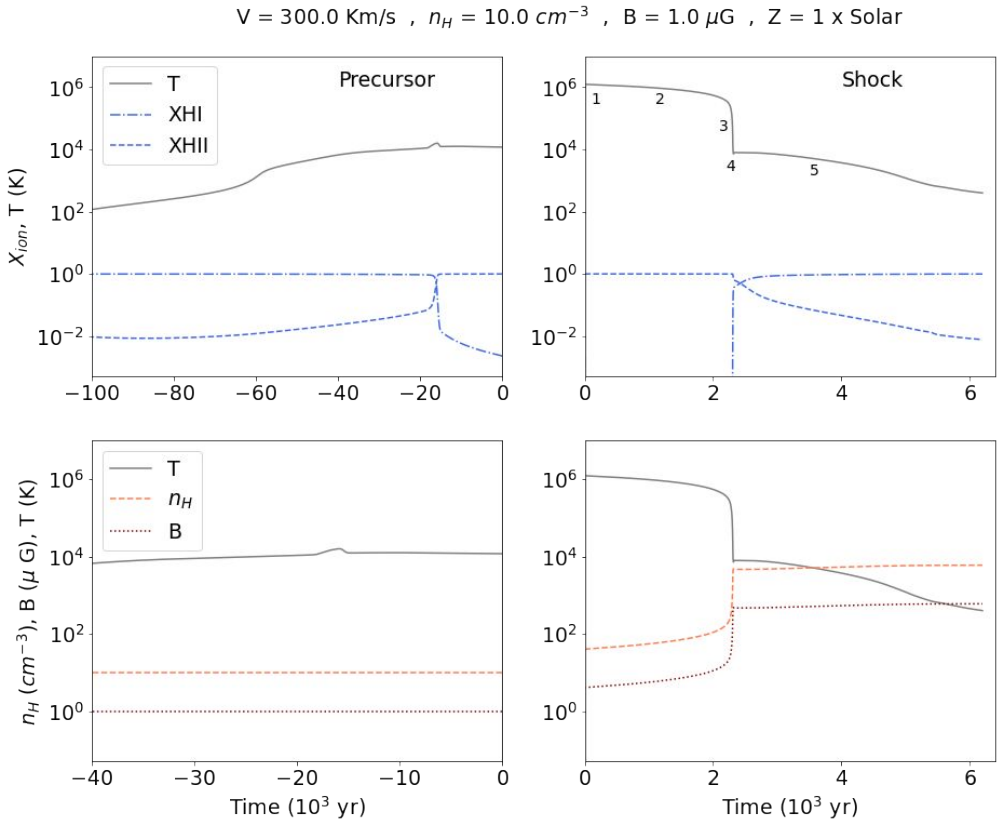
The ionization front is supersonic in the pre-shock medium.

Shock Parameters

Velocity
Pre-shock density
Magnetic field
Metallicity



MAPPINGS models



UV Luminosity

$$L_{uv} = 2.22 \times 10^{-10} \cdot V^{3.02} \cdot n_H \quad [erg\, cm^{-2}\, s^{-1}]$$

Compression factor: R

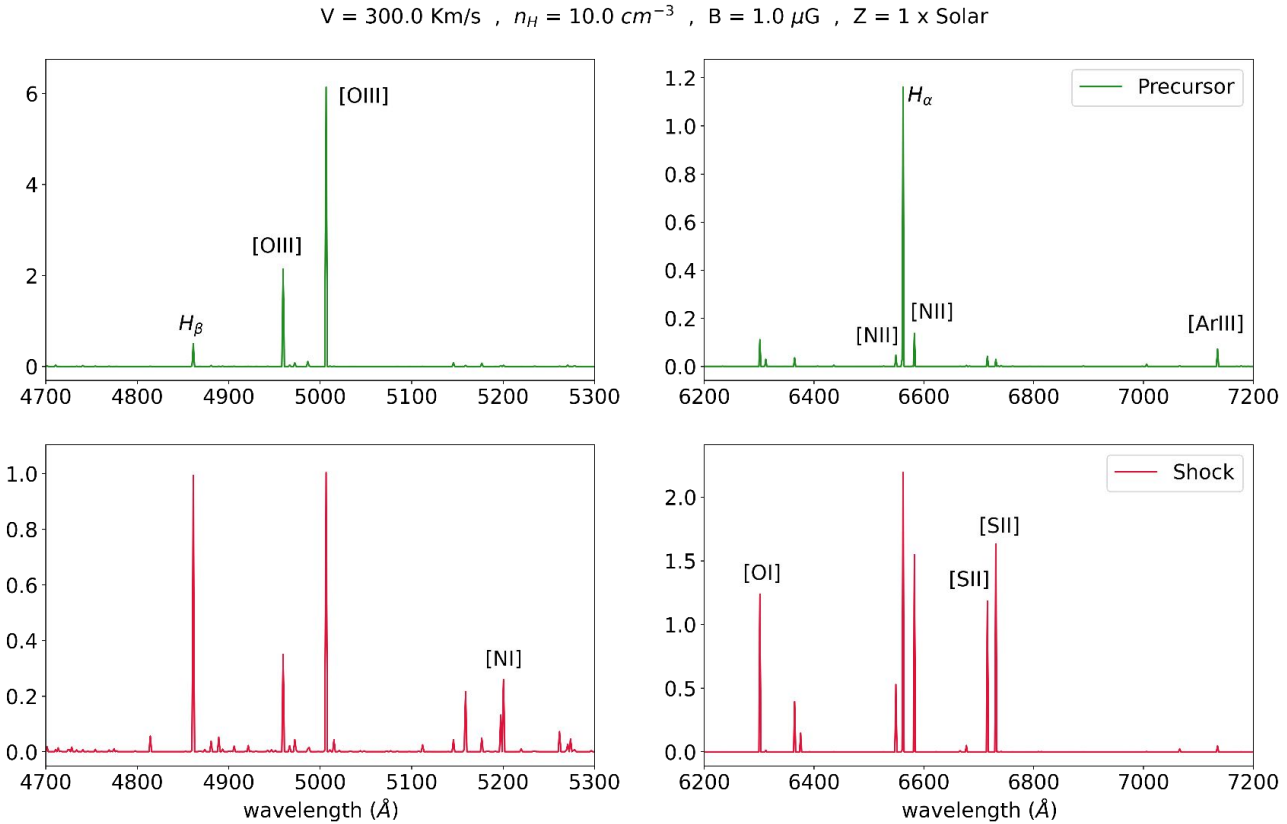
$$R_n = \sqrt{2} \cdot M_a$$

$$M_a \approx 2.75 \times 10^{-2} \cdot V \cdot n_H^{1/2} \cdot B^{-1}$$

MAPPINGS models

Model spectra

Hβ , Hα
[OIII] λ 5007
[NII] λλ 6548, 84
[SII] λλ 6717,31
[SIII] λ 9069
[OI] λ 6300
[NI] λλ 5198, 5200
[ArIII] λ 7137



Observations

PHANGS Catalog

ALMA + HST + MUSE + JWST

Radio + Ultraviolet + Optical + Infrared

Table 1. General properties of the PHANGS-MUSE sample.

Name	Distance[a] [Mpc]	Log($M_\star$)[b] [$M_\odot$]	Log(SFR)[b] [$M_\odot$ yr^{-1}]	Δ_{SFMS}[b] [dex]	R_{25}[c] [arcmin]	PA[d] [deg]	i[d] [deg]	scale [pc/arcsec]	PSF[e] [arcsec]	copt PSF[f] [arcsec]
IC5332	9.0	9.67	-0.39	0.01	3.0	74.4	26.9	43.7	$0.72\pm^{0.08}_{0.12}$	0.87
NGC0628	9.8	10.34	0.24	0.18	4.9	20.7	8.9	47.7	$0.73\pm^{0.13}_{0.11}$	0.92
NGC1087	15.9	9.93	0.12	0.33	1.5	359.1	42.9	76.8	$0.74\pm^{0.10}_{0.12}$	0.92
NGC1300	19.0	10.62	0.07	-0.18	3.0	278.0	31.8	92.1	$0.63\pm^{0.18}_{0.13}$	0.89
NGC1365	19.6	10.99	1.23	0.72	6.0	201.1	55.4	94.9	$0.82\pm^{0.26}_{0.24}$	1.15
NGC1385	17.2	9.98	0.32	0.50	1.7	181.3	44.0	83.5	$0.49\pm^{0.10}_{0.11}$	0.77
NGC1433	18.6	10.87	0.05	-0.36	3.1	199.7	28.6	90.3	$0.65\pm^{0.18}_{0.14}$	0.91
NGC1512	18.8	10.71	0.11	-0.21	4.2	261.9	42.5	91.3	$0.80\pm^{0.38}_{0.16}$	1.25
NGC1566	17.7	10.78	0.66	0.29	3.6	214.7	29.5	85.8	$0.64\pm^{0.09}_{0.10}$	0.80
NGC1672	19.4	10.73	0.88	0.56	3.1	134.3	42.6	94.1	$0.72\pm^{0.17}_{0.08}$	0.96
NGC2835	12.2	10.00	0.09	0.26	3.2	1.0	41.3	59.2	$0.85\pm^{0.23}_{0.18}$	1.15
NGC3351	10.0	10.36	0.12	0.05	3.6	193.2	45.1	48.3	$0.74\pm^{0.24}_{0.13}$	1.05
NGC3627	11.3	10.83	0.58	0.19	5.1	173.1	57.3	54.9	$0.77\pm^{0.21}_{0.10}$	1.05
NGC4254	13.1	10.42	0.49	0.37	2.5	68.1	34.4	63.5	$0.58\pm^{0.23}_{0.14}$	0.89
NGC4303	17.0	10.52	0.73	0.54	3.4	312.4	23.5	82.4	$0.58\pm^{0.12}_{0.07}$	0.78
NGC4321	15.2	10.75	0.55	0.21	3.0	156.2	38.5	73.7	$0.64\pm^{0.45}_{0.18}$	1.16
NGC4535	15.8	10.53	0.33	0.14	4.1	179.7	44.7	76.5	$0.44\pm^{0.03}_{0.01}$	0.56
NGC5068	5.2	9.40	-0.56	0.02	3.7	342.4	35.7	25.2	$0.73\pm^{0.23}_{0.21}$	1.04
NGC7496	18.7	10.00	0.35	0.53	1.7	193.7	35.9	90.8	$0.79\pm^{0.03}_{0.17}$	0.89



Emsellem et. al. (2022)

NGC 1566

Machine Learning Classification

PHANGS Data Set

Emission lines

Hβ , Hα
[OIII] λ 5007
[NII] λλ 6548, 84
[SII] λλ 6717,31

spaxel-by-spaxel

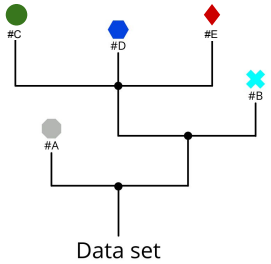
Normalization

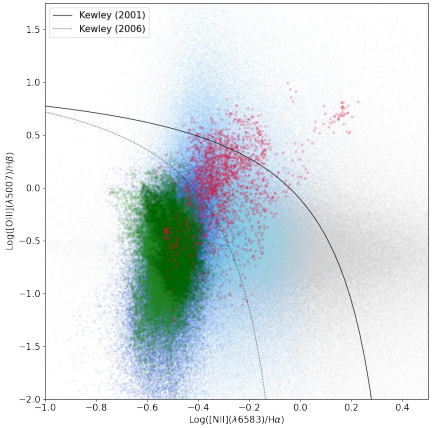
$$F = \frac{Log(f)}{Max(\,Log(f)\,)}$$

Machine learning clustering algorithm

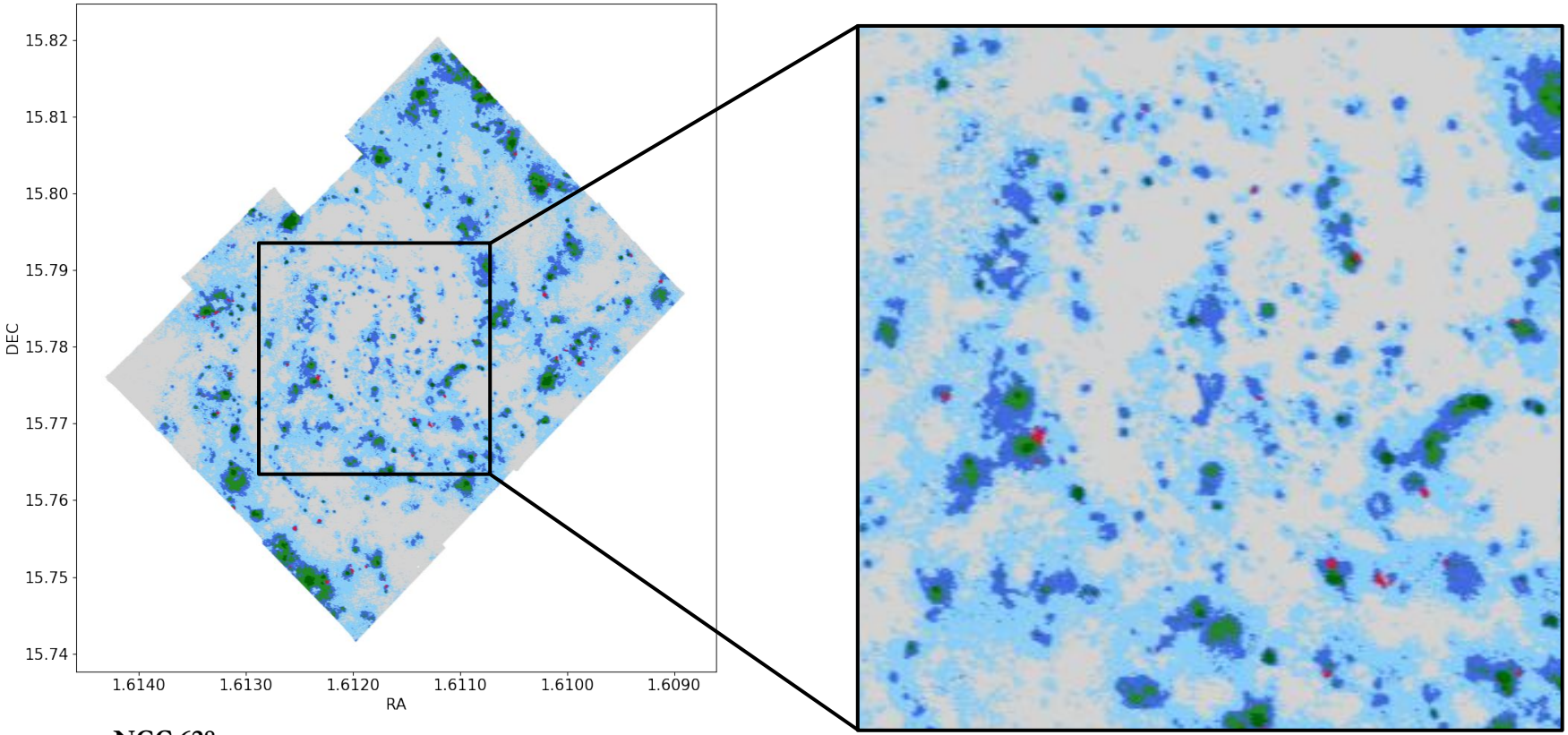
Unsupervised Bayesian Gaussian Mixture Model

Physical Interpretation



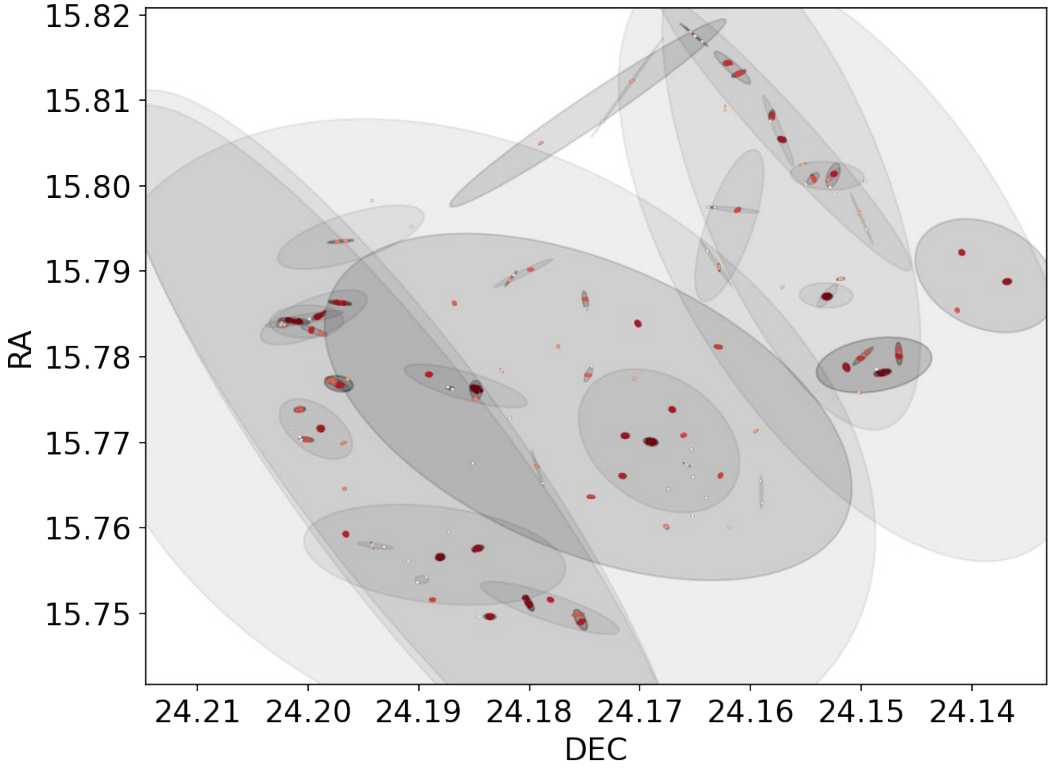


Machine Learning Classification



NGC 628

PHANGS Catalog



NGC 628

ML Algorithm

BDSCAN

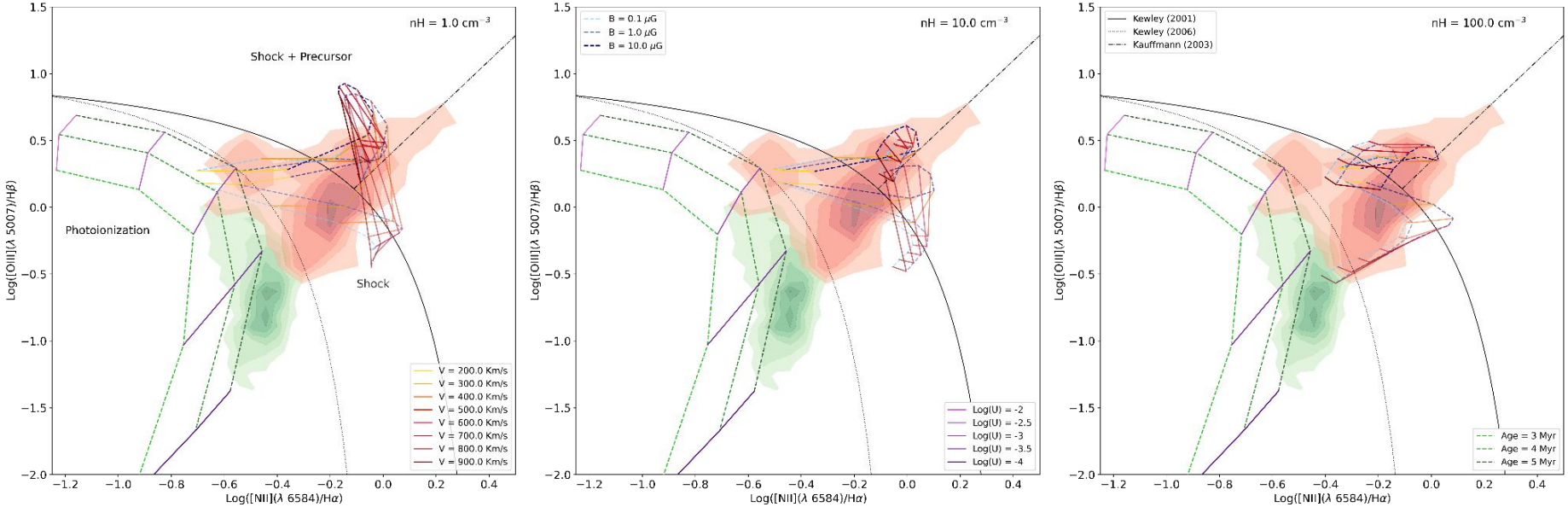
Density-Based Spatial Clustering of Applications with Noise

Final Catalog

HII Regions	2210
SNR	483

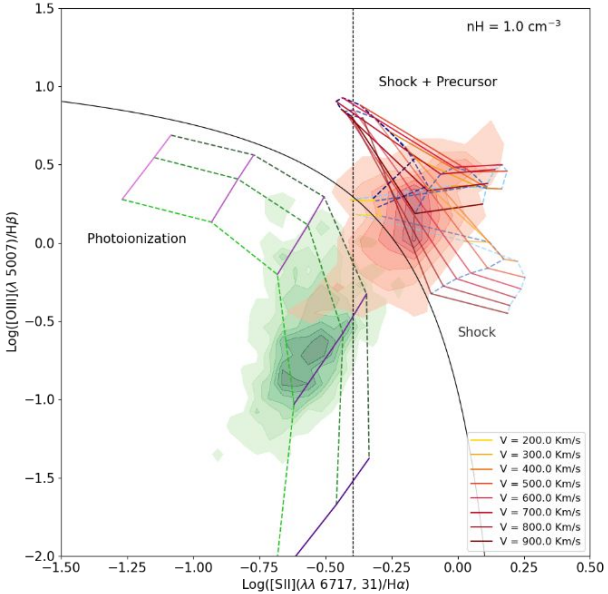
Diagnostic Diagrams

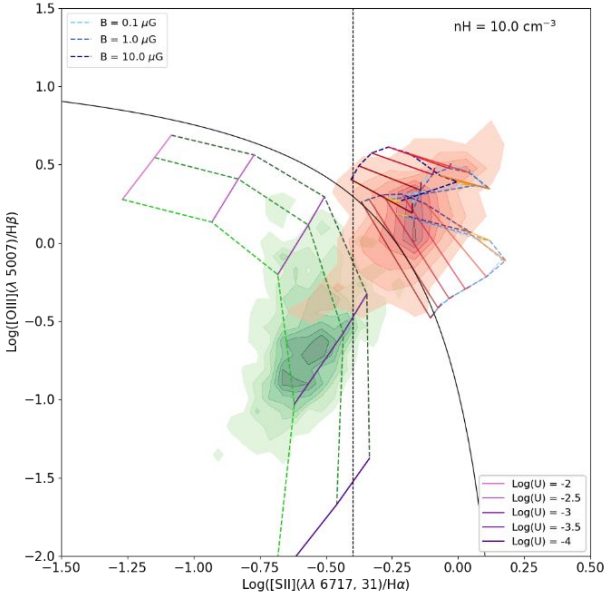
Diagnostic Diagrams

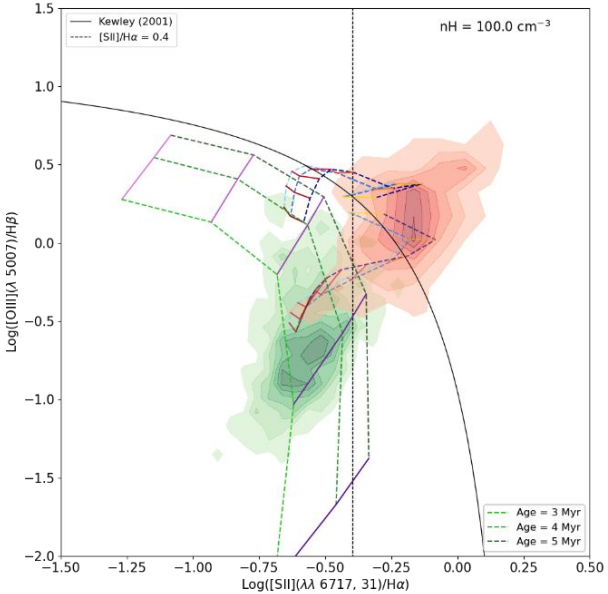


$[OIII]/H\beta$ Vs $[NII]/H\alpha$

Diagnostic Diagrams

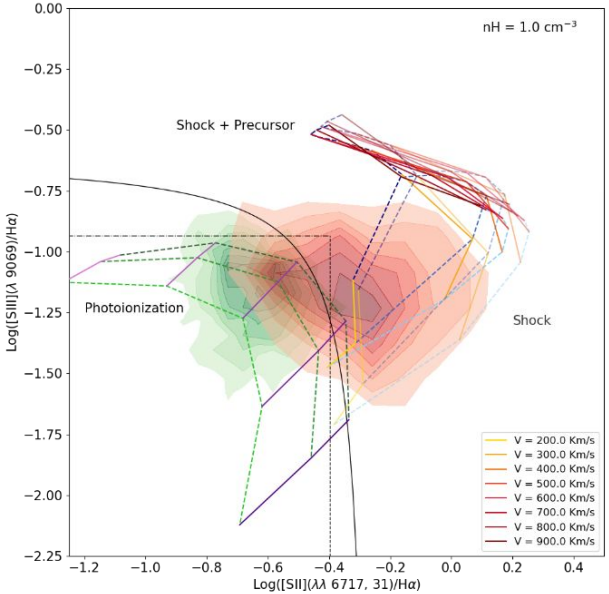


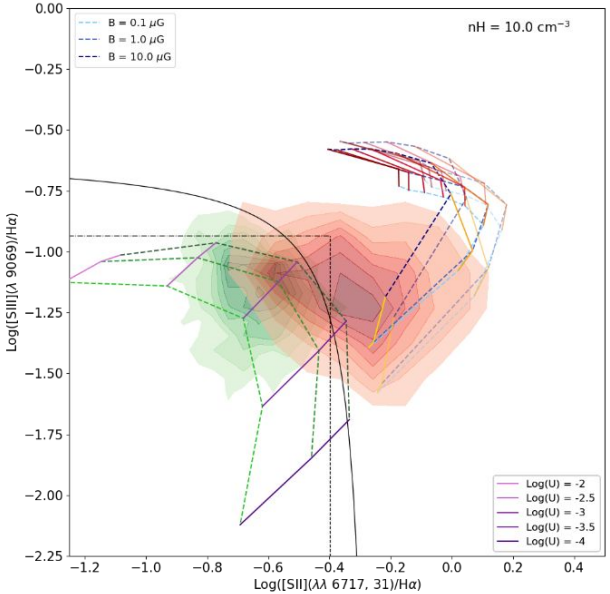


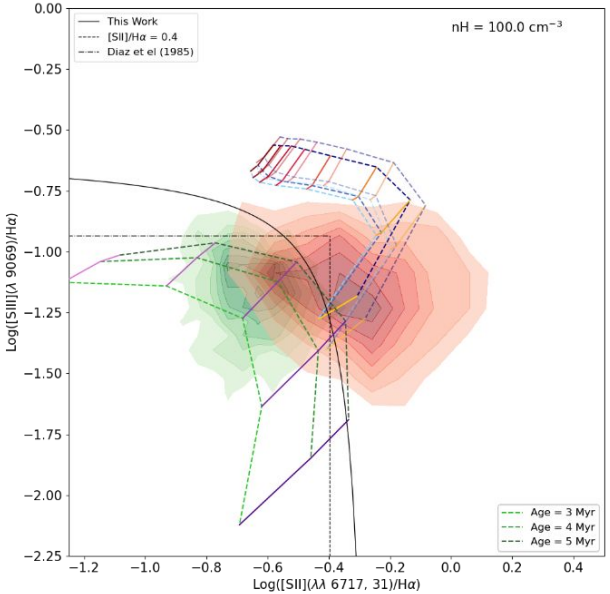


$[OIII]/H\beta$ Vs $[SII]/H\alpha$

Diagnostic Diagrams

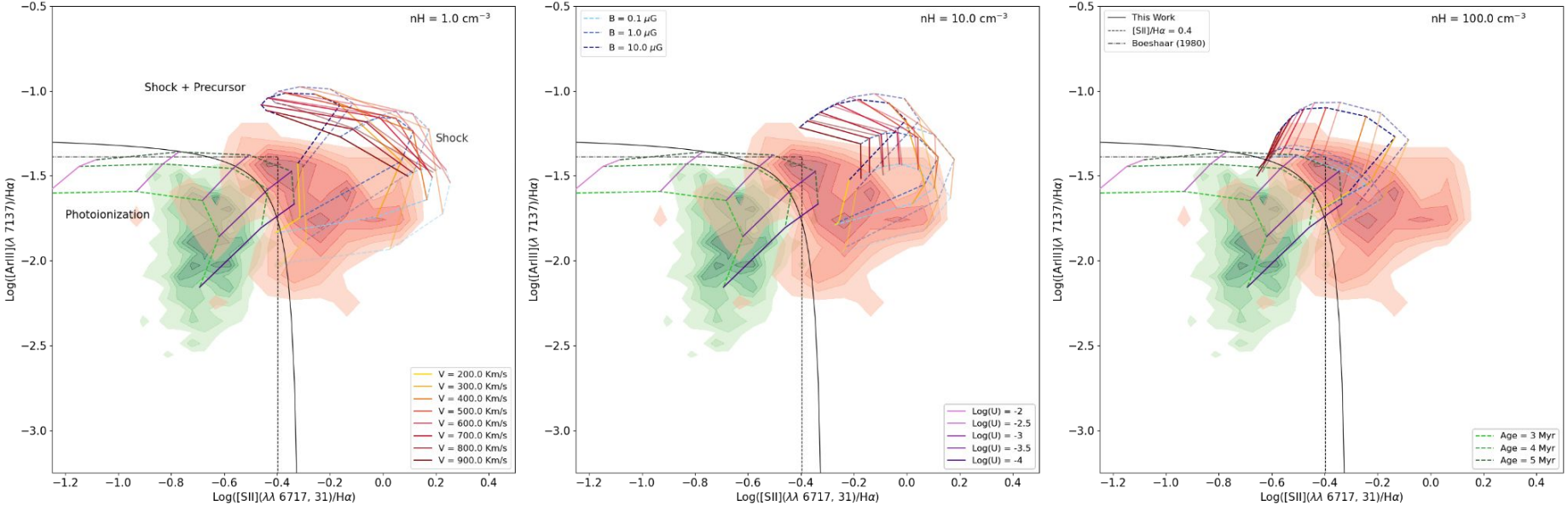






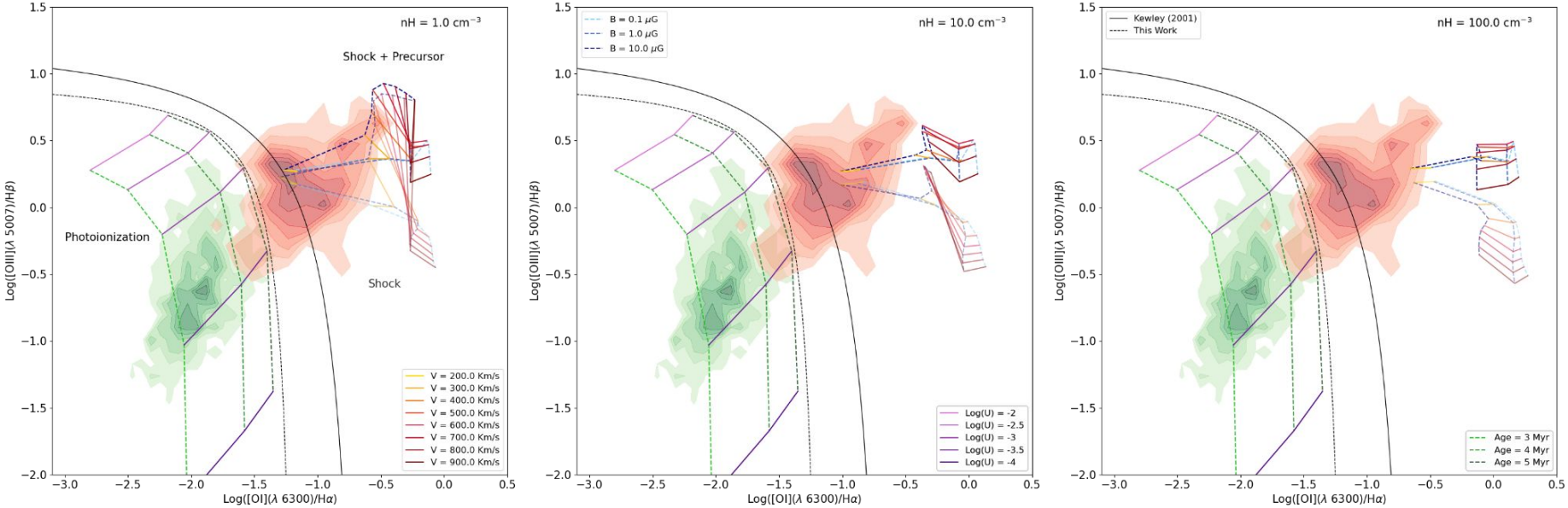
$[SIII]/H\alpha$ Vs $[SII]/H\alpha$

Diagnostic Diagrams



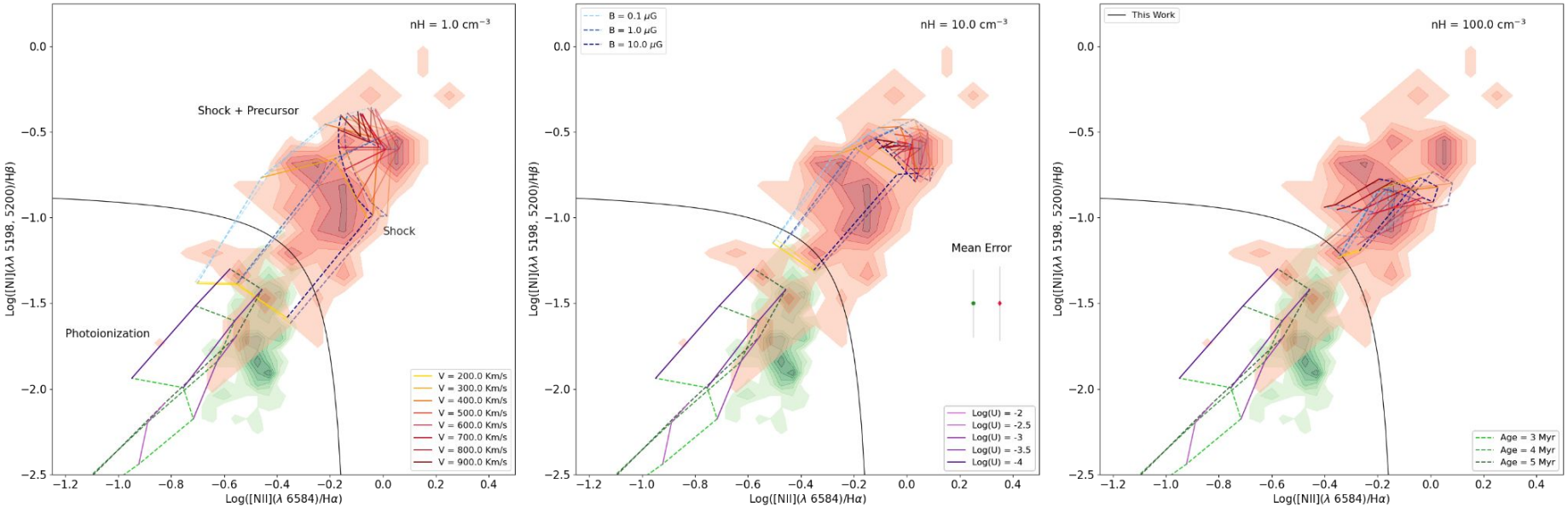
$[ArIII]/H\alpha$ Vs $[SII]/H\alpha$

Diagnostic Diagrams



$[OIII]/H\beta$ Vs $[OI]/H\alpha$

Diagnostic Diagrams

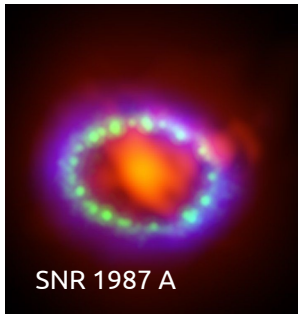


$[NI]/H\beta$ Vs $[NII]/H\alpha$

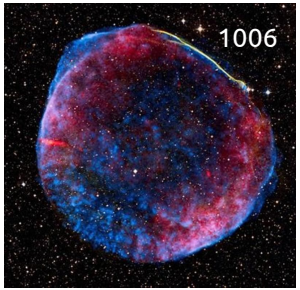
SNR Evolution

Supernova Remnants

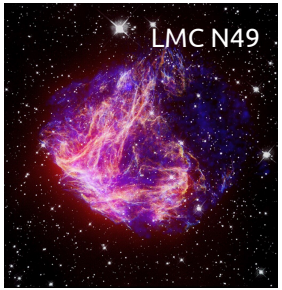
Evolution



Ejecta - Dominated
Free Expansion



Sedov-Taylor



Pressure-Driven
Snow-Plough

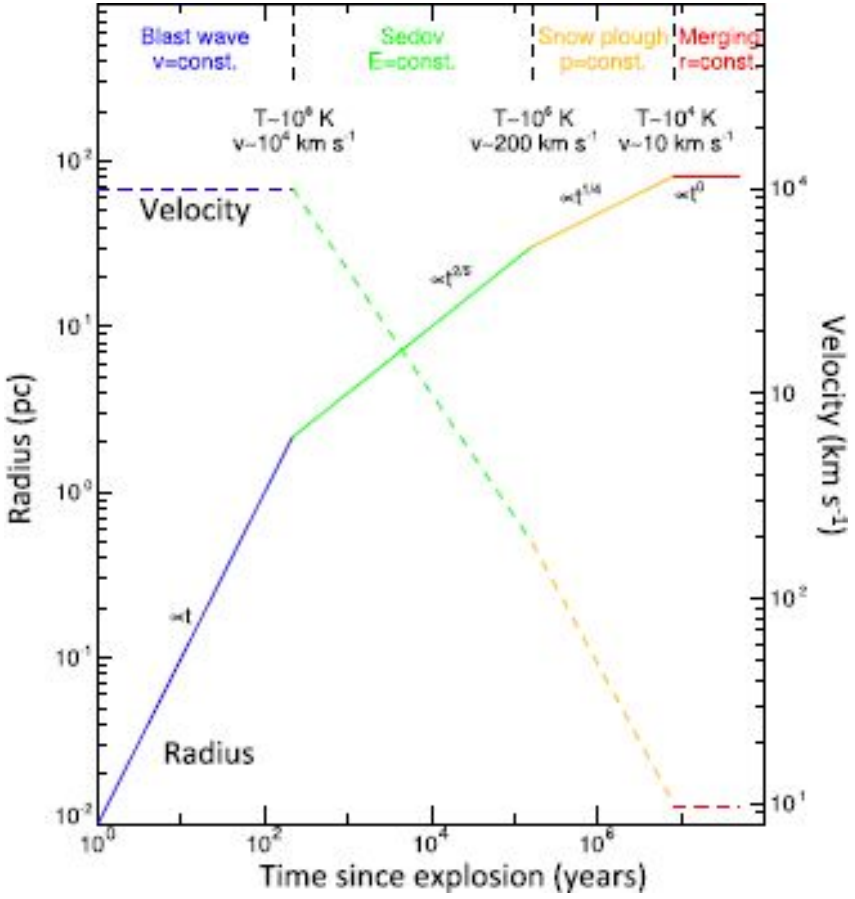


Merging Phase

Non-Radiative

Radiative

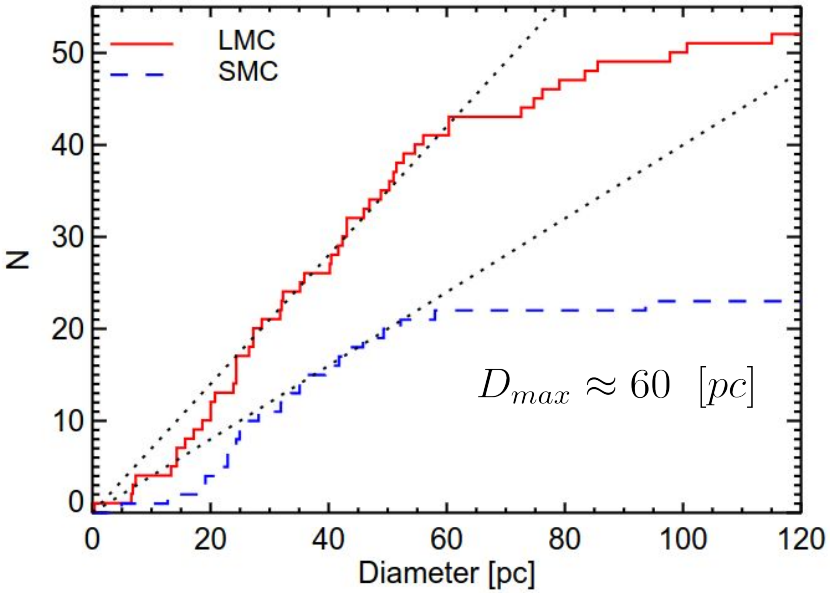
Supernova Remnants Evolution

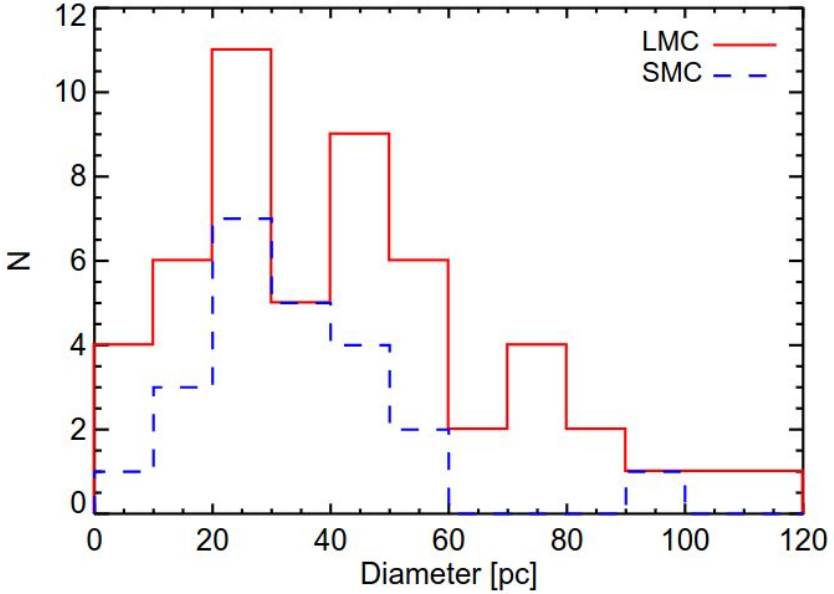


Padmanabha (2001)
Wilms (2012)

SNR Size Distribution

Sedov - Taylor





Badenes, Maoz & Draine (2010)

SNR Size Distribution

Sedov - Taylor

To

Pressure - Driven

$$R_0 = 14.0 \cdot E_{51}^{2/7} \cdot n_o^{-3/7} \cdot \zeta^{-1/7}\, pc$$

$$V_0 = 413 \cdot E_{51}^{1/14} \cdot n_o^{1/7} \cdot \zeta^{3/14}\, Km/s$$

$$t_0 = 1.33 \times 10^4 \cdot E_{51}^{3/14} \cdot n_o^{-4/7} \cdot \zeta^{-5/14}\, Yr$$

Pressure - Driven

Evolution

$$R = R_0 \cdot \left(\frac{4}{3} t_* - \frac{1}{3}\right)^{3/10}$$

$$V = V_0 \cdot \left(\frac{4}{3} t_* - \frac{1}{3}\right)^{-7/10}$$

Bisnovaty (1995)
Blondin (1998)
Truelove & McKee (1999)

SNR Size Distribution

Pressure - Driven

Evolution

$$R = R_0 \cdot \left(\frac{4}{3} t_* - \frac{1}{3}\right)^{3/10}$$

$$V = V_0 \cdot \left(\frac{4}{3} t_* - \frac{1}{3}\right)^{-7/10}$$

Single:

$$\frac{dN}{dR} = \frac{dN}{dt}\,\frac{dt}{dR}$$

$$\frac{dN}{dt} = cte$$

$$\frac{dN}{dR} \propto R^{7/3}$$

SNR Size Distribution

Single:

$$\frac{dN}{dR} = \frac{dN}{dt}\,\frac{dt}{dR}$$

$$\frac{dN}{dt} = cte$$

$$\frac{dN}{dR} \propto R^{7/3}$$

Environmental Effects

$$\frac{dN}{dR} \propto R^{7/3} \cdot \int_{n_{o,min}}^{n_{o,max}} n_o^{6/7}\,\frac{dP}{dn_o}\,dn_o$$

$$\frac{dP}{dn_o} \propto n_o^{\beta}$$
$$\beta = -1$$

$$R_{max} = 4.93 \cdot R_0 \cdot \left(\frac{E_{51}^{1/14} \cdot n_o^{1/7} \cdot \zeta^{3/14}}{M \cdot C_{o,6}}\right)^{3/7}$$

Cioffi (1988)

SNR Size Distribution

Single:

$$\frac{dN}{dR} = \frac{dN}{dt}\frac{dt}{dR}$$

$$\frac{dN}{dt} = cte$$

$$\frac{dN}{dR} \propto R^{7/3}$$

Environmental Effects

$$\frac{dN}{dR} \propto R^{\frac{-49}{18}\cdot\left(\beta+\frac{13}{7}\right)+\frac{7}{3}}$$

$$\frac{dP}{dn_o} \propto n_o^{\beta}$$
$$\beta = -1$$

$$\frac{dN}{dR} \propto R^{0}$$

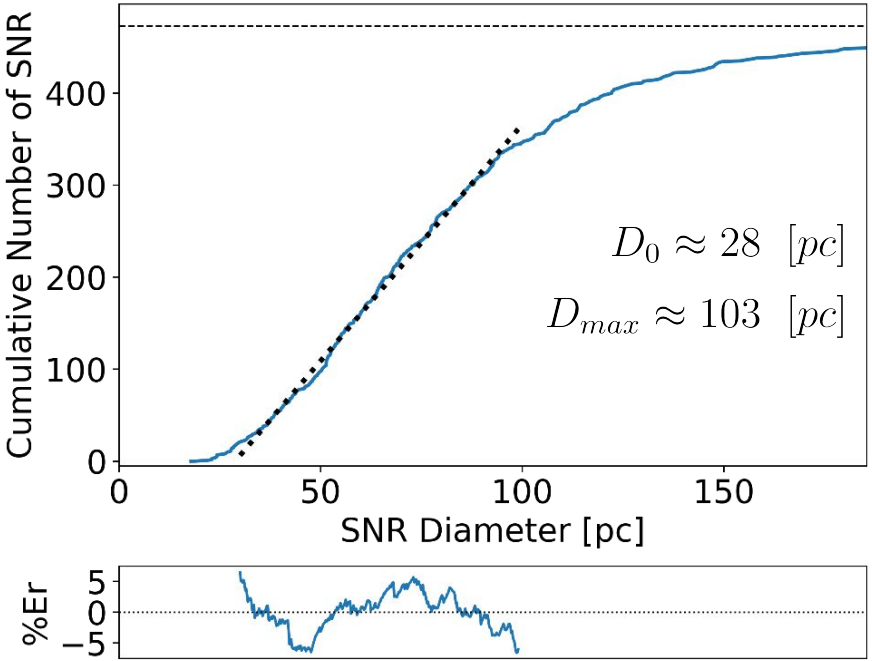
$E_{51} = 1 \qquad n_o = 1$
$C_{o,6} = 1 \qquad \zeta = 1$
$M = 2$

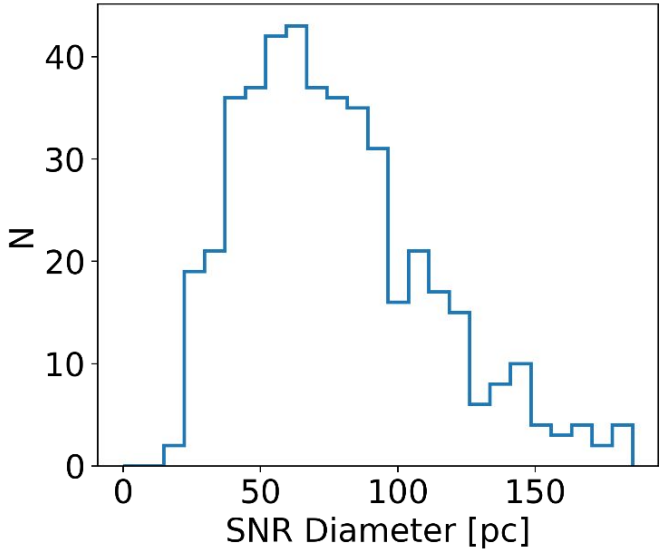
Typical SNR

$R_0 \simeq 14.0\,[pc]$
$R_{max} \simeq 51.3\,[pc]$

SNR Size Distribution

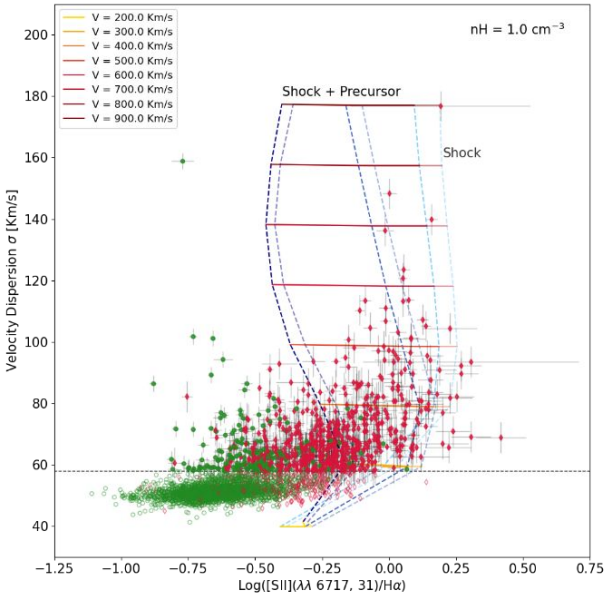
My Work

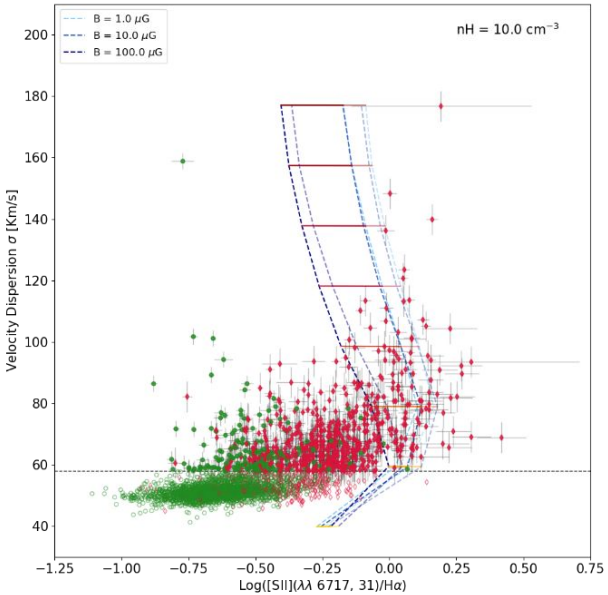


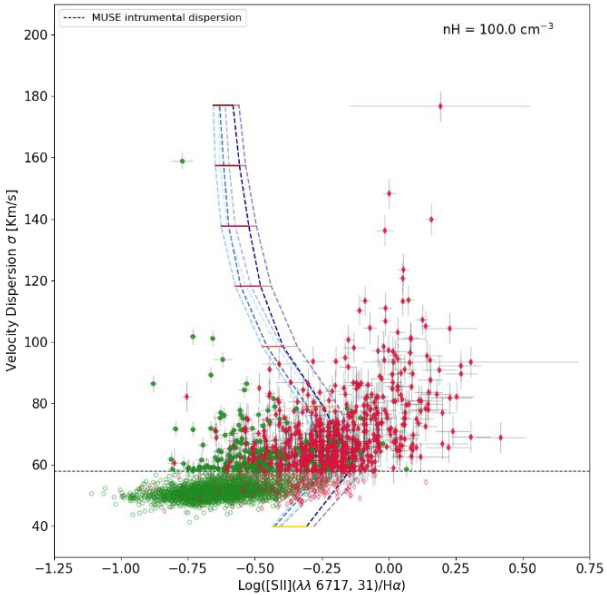


Kinematics

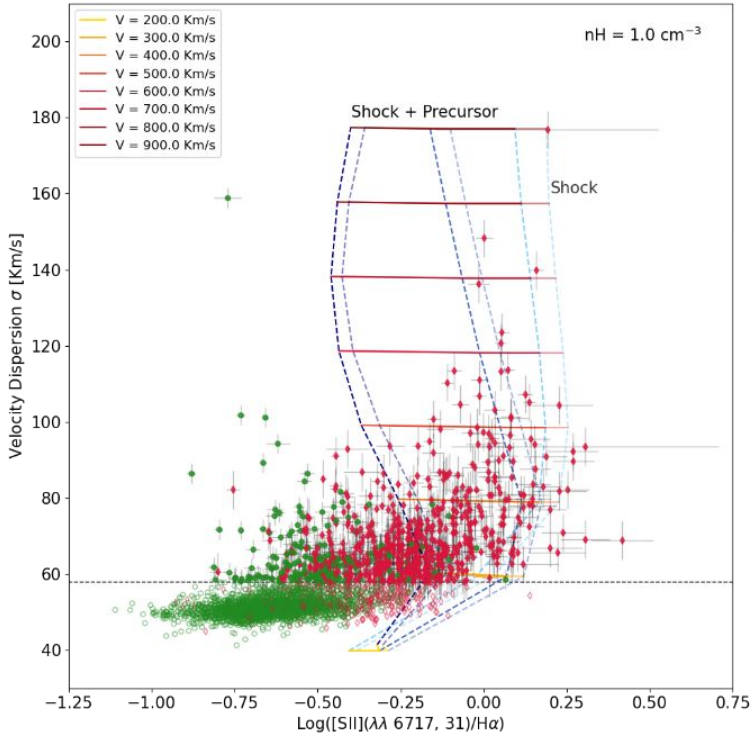
Supernova Remnants Kinematics



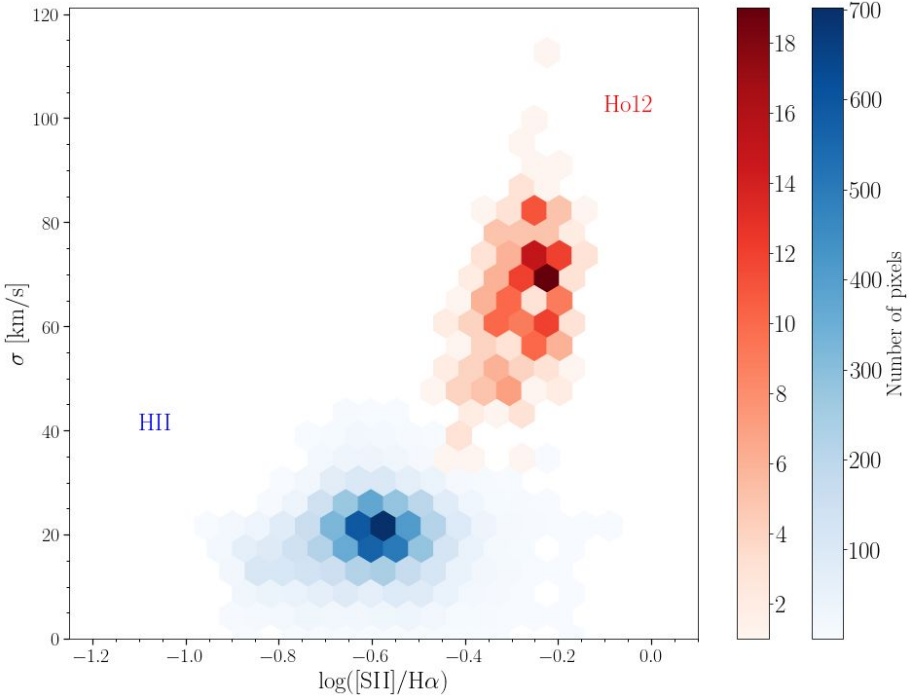




Supernova Remnants Kinematics



Duarte - Puertas
(Yesterday)



Great minds think alike

Conclusions

Conclusions

- Our machine Learning Algorithm is able to find the SNR population in nearby galaxy in a systematic and unbiased way.
- Our SNR are in good agreement with the MAPPINGS emission models.
- We need different diagnostic diagrams to explore the SNR population and new analysis to obtain the functional parameters. (Velocity, Density, Magnetic field and Metallicity)
- The observe size distribution is in good agreement with our understanding of radiative pressure-driven SNR.
- MUSE it is insufficient for an in deep kinematic analysis, but SITELLE it is not.



Thanks

This research has been funded by grants
PID2022-136598NB-C31, C32, and C33

The wokshop has been funded by grant
PID2019-107408GB-C41

all grants are funded by
MCIN/AEI/10.13039/501100011033 and by "ERDF A way of making Europe"